0026-895X/96/051295-14$3.00/0

MOLECULAR PHARMACOLOGY, 50:1295–1308 (1996).

Regulation of D_2 Dopamine Receptors by Amiloride and Amiloride Analogs

S. R. J. HOARE and P. G. STRANGE

Research School of Biosciences, Biological Laboratory, The University, Canterbury, CT2 7NJ, UK

Received November 10, 1996; Accepted June 11, 1996

SUMMARY

Allosteric regulation of rat D_2 dopamine receptors by amiloride and amiloride analogs has been studied by investigating their ability to accelerate the dissociation of [^{3}H]spiperone from the receptors expressed in Ltk$^-$ cells. The amiloride analogs were more potent and produced a greater maximal effect on the rate of [^{3}H]spiperone dissociation than did amiloride. [^{3}H]Spiperone dissociation was biphasic and could be resolved into contributions from fast and slow rates in the absence and presence of the modulators. Methylisobutylamiloride accelerated both the fast and slow rates of dissociation and modulated the proportions of the two rates. The association of [^{3}H]spiperone in the absence of modulators was also biphasic. The combination of the two sets of association and dissociation rate constants gave very similar equilibrium dissociation constants, and this was confirmed in equilibrium binding experiments that were consistent with a single binding site. It is proposed that there are two binding states for [^{3}H]spiperone that can be distinguished kinetically but not in equilibrium binding experiments. The proportions of these states are differentially modulated with the use of sodium ions and magnesium ions, whereas GTP has no significant effect. Allosteric regulation of [^{3}H]spiperone binding by methylisobutylamiloride could also be observed in saturation and inhibition binding experiments. These effects can be accounted for in a model in which the modulator binds to the competitive site of the receptor and to an allosteric site on the receptor from which it exerts negatively cooperative effects on [^{3}H]spiperone binding to the competitive site and positively cooperative effects on the binding of the modulator to the competitive site.

The D_2 dopamine receptor is a member of the large family of receptors that activate G proteins and are thought to contain seven α helical membrane-spanning domains. Several members of this family of G protein-coupled receptors have been shown to be regulated allosterically. For example, allosteric inhibition of ligand binding is exhibited by a diverse group of compounds that interact with muscarinic acetylcholine receptors (for a review, see Ref. 1). The interaction of gallamine with this class of receptors has been characterized in detail (2–4). The five known muscarinic receptor subtypes are regulated with varying potencies by this compound (5, 6), with the most potent interaction occurring at the M_2 receptor and the least potent (by 100-fold) occurring at the M_5 subtype (6). Allosteric enhancement has been demonstrated for a series of 2-amino-3-benzoylthiophene ligands that act at the adenosine A_1 receptor (7, 8). These compounds enhance the binding and function of agonist ligands (7, 9). The flexible nature of these interactions, together with the potential for subtype selectivity, make allosteric sites attractive for therapeutic intervention (10, 11). However, to develop allosteric modulators into effective therapies, their mechanism of action must be carefully elucidated (12).

Like other receptors that are linked to the attenuation of adenylyl cyclase, ligand binding to the D_2 dopamine receptor and α_2-adrenergic receptor is regulated by Na^+ and pH (13, 14). In addition, ligand binding to these receptors has been shown to be allosterically regulated by amiloride and analogs of this compound (13, 14). Amiloride interacts with a number of cation-binding proteins (15), so it was thought that the regulation of these receptors by amiloride and cations might be associated. A conserved aspartate residue, which lies in the second putative transmembrane domain, has been shown to be the site involved in sodium regulation of the α_2-adrenergic receptor (Asp79) (16) and the D_2 dopamine receptor (Asp80) (17). In the α_2-adrenergic receptor, however, mutation of this residue completely removed the allosteric effects of Na^+ on ligand binding without perturbing allosteric regulation by amiloride analogs (16). It has also been suggested that regulation of receptors by Na^+, pH, and amiloride analogs may be a manifestation of the ability of these receptors to affect Na^+/H^+ exchange (13, 14).

We thank the Biotechnology and Biological Sciences Research Council and SmithKline Beecham pharmaceuticals for financial support.

ABBREVIATIONS: DMA, dimethylamiloride; EIA, ethylisopropylamiloride; HMA, hexamethyleneamiloride; MIA, methylisobutylamiloride; NMDG, *N*-methyl-D-glucamine; DMSO, dimethylsulfoxide; EGTA, ethylene glycol bis(β-aminoethyl ether)-*N*,*N*,*N*′,*N*′-tetraacetic acid; HEPES, 4-(2-hydroxyethyl)-1-piperazineethanesulfonic acid.

Amiloride and analogs of this compound have also been shown to affect equilibrium radioligand binding to the D_2 dopamine receptor (13) and the α_2-adrenergic receptor (18). In this study, we examined the regulation of [^{3}H]spiperone binding to D_2 dopamine receptors by amiloride and analogs of amiloride in kinetic and equilibrium assays to understand the nature of the allosteric regulation involved. Models have been formulated to describe quantitatively the regulation of [^{3}H]spiperone binding in the equilibrium assays. In these models, the modulator binds to an allosteric site on the receptor from which it regulates its own binding and the binding of the radioligand to the competitive binding site.

Experimental Procedures

Materials. [^{3}H]Spiperone (15–30 Ci/mmol) was purchased from Amersham International (Buckinghamshire, UK). Amiloride was obtained from Sigma Chemical (Poole, Dorset, UK). Benzamil, DMA, EIA, MIA, HMA, and (+)-butaclamol were purchased from Research Biochemicals (Natick, MA). All other materials were obtained from commercial sources and were of the highest available purity.

Cell growth. Ltk59 cells (19) expressing the rat $D_{2(long)}$ dopamine receptor were adapted for growth in suspension. Frozen stocks of cells (1 ml of 2×10^6 cells/ml) previously grown as adherent monolayers (19) were thawed and resuspended in 20 ml of RPMI medium supplemented with 2 mM glutamine, 5% fetal bovine serum, and 200 μg/ml active geneticin. The cells, which were maintained in an atmosphere of 5% CO_2 at 37°, were initially grown in Erlenmyer flasks on an orbital shaker set at 100 rpm before transfer into stirrer bottles designed for suspension culture. Cells were added to stirrer bottles at a final density of $\sim 2 \times 10^5$ cells/ml and grown to a final density of 7×10^5 to 1×10^6 cells/ml. The bottles were incubated on magnetic stirrers set at 70 rpm.

Preparation of cell membranes. Ltk59 cells were centrifuged at 3800 × *g* for 20 min at 4°. The cell pellet was then washed with an ice-cold buffer containing 20 mM HEPES, 1 mM EDTA, 1 mM EGTA, and 6 mM $MgCl_2$, pH 7.4, and centrifuged as before. Washed cells were resuspended in buffer ($\sim 1 \times 10^9$ cells in 30 ml of buffer). The cells were lysed by sonication using an MSE 150-W Ultrasonic Disintegrator. Aliquots of 30 ml of washed cells were placed in a beaker of ice and subjected to six 5-sec pulses (18 μm and 3 mm diameter exponential probe) separated by 5-sec intervals to avoid heating the lysate. Lysates were then centrifuged at 1,700 × *g* for 10 min at 4°. The supernatant from sonication lysates was centrifuged at 48,000 × *g* for 1 hr at 4°. The resulting membrane pellets were resuspended in assay buffer [20 mM HEPES, 1 mM EDTA (free acid), 1 mM EGTA (free acid), pH 7.4] and stored in 1-ml aliquots at −80°.

Measurement of [^{3}H]spiperone dissociation. Allosteric interactions were detected using radioligand dissociation assays. Dissociation of [^{3}H]spiperone was measured using the unlabeled drug method. Membranes (40–100 μg) were preincubated with 0.25 nM [^{3}H]spiperone, in a total volume of 0.9 ml of assay buffer for 1 hr at 25°. In some experiments, the buffer contained 6 mM $MgCl_2$; this is indicated in the text where appropriate. The effects of GTP (100 μM) were measured using buffer containing 6 mM $MgCl_2$. Radioligand dissociation was then initiated by the addition of a saturating concentration of (+)-butaclamol (3 μM) with or without allosteric modulators. Amiloride analogs were dissolved in DMSO, whereas amiloride was soluble in distilled water. The final DMSO concentration was ≤0.75%, and the appropriate vehicle was added in control experiments. The time course of dissociation of total binding was measured by rapid filtration of triplicate aliquots at appropriate time intervals. The samples were filtered through Whatman GF/C glass-fiber filters on a Brandel cell harvester with four washes of 3 ml of phosphate-buffered saline (0.14 M NaCl, 3 mM KCl, 1.5 mM KH_2PO_4, 5 mM Na_2HPO_4, pH 7.4). Filters were then soaked for ≥6 hr in 2 ml of LKB Optiphase Hisafe 3 scintillation fluid before determination of radioactivity by liquid scintillation counting. Nonspecific binding was measured after a 1-hr incubation in the presence of 3 μM (+)-butaclamol.

Measurement of [^{3}H]spiperone association. Membranes (20–30 μg in 0.9 ml of assay buffer) and [^{3}H]spiperone were brought to 25° by incubating them separately for 20 min. In some experiments, the buffer contained 6 mM $MgCl_2$, 120 mM NaCl, or 120 mM NMDG. In experiments designed to measure the effects of GTP, the modulator was present at a concentration of 100 μM in a buffer containing 6 mM $MgCl_2$. Association was initiated by the addition of 0.1 ml [^{3}H]spiperone, producing a final radioligand concentration of 0.2–0.4 nM. Bound and free radioligands were separated, and filter-bound radioactivity was measured as described for measurement of dissociation. The bound radioligand varied from 5% to 12% of the free radioligand concentration.

Inhibition of equilibrium binding of [^{3}H]spiperone by MIA. In these experiments, the binding of a fixed concentration of [^{3}H]spiperone was measured in the presence of a range of concentrations of MIA. Cell membranes (30–60 μg) were incubated with [^{3}H]spiperone (0.15–0.2 nM) and a range of concentrations of MIA in 1 ml of assay buffer at 25° for 2 hr. Triplicate determinations at each concentration of MIA were performed. Total binding was measured in the presence of 0.75% DMSO. Nonspecific binding was measured in the presence of the solvent and 3 μM (+)-butaclamol.

Saturation analysis of [^{3}H]spiperone binding. These experiments were performed to determine the K_d and B_{max} of [^{3}H]spiperone binding. A large assay volume (10 ml) was used to obtain an accurate measure of K_d (see below). The effect of MIA on [^{3}H]spiperone saturation parameters was measured using an assay volume of 1 ml. Because this latter procedure may produce erroneous estimates of K_d, the effect of a well-characterized ligand [haloperidol (a competitive antagonist)] on K_d and B_{max} was also determined.

Large-volume saturation experiments were carried out in a volume of 10 ml, so that a low concentration of membranes could be used. If high concentrations of membranes are used, the lipophilic nature of [^{3}H]spiperone can result in erroneous estimates of affinity because of the ligand depletion caused by binding to receptors and because of partitioning into the lipid phase of the membrane (20). Membranes (30–45 μg) were incubated at 25° with 12–18 concentrations of [^{3}H]spiperone (total concentrations were typically 1 pM to 1 nM) with triplicate or quadruplicate measurements. An association assay indicated that a total [^{3}H]spiperone concentration of 9 pM reached equilibrium in 4 hr. To ensure that incubations of lower radioligand concentrations had attained equilibrium, an 8-hr incubation period was used. Total and nonspecific bindings were measured in the presence of 3 μM (−)-butaclamol and 3 μM (+)-butaclamol, respectively. Filtration was carried out as before, except that four washes of 6 ml were used, which was found to be sufficient to wash the filters in a preliminary experiment. The total receptor concentration in these assays varied between 0.9 and 2.2 pM.

For small-volume saturation experiments, cell membranes (50–60 μg) were incubated with a range of concentrations of [^{3}H]spiperone (total concentrations were typically 10 pM to 1 nM for experiments in the absence of modulators) in a final volume of 1 ml at 25°. Radioligand association experiments demonstrated that in the presence of 0.75% DMSO, 10 μM MIA, or 31.6 μM MIA, total [^{3}H]spiperone concentrations of 20–40% of K_d reached equilibrium with the receptor within 2 hr. To ensure that lower concentrations of [^{3}H]spiperone had equilibrated, an incubation period of 4 hr was used. Total binding was measured in the presence of 3 μM (−)-butaclamol, whereas nonspecific binding was determined by incubation with 3 μM (+)-butaclamol. In experiments that included MIA or haloperidol, the range of [^{3}H]spiperone concentrations was varied according to apparent K_d values obtained in initial experiments. Each measurement was performed in triplicate. The total receptor concentration in these experiments was 38–72 pM.

Data analysis. Dissociation and association data were analyzed using the KINETIC program of LIGAND (Biosoft, Ferguson, MO).

The EBDA and LIGAND programs of this package were used to analyze pseudocompetition and saturation data. Concentration-dependence isotherms were analyzed using InPlot (GraphPAD Software, San Diego, CA). For comparison of the allosteric effects of the different compounds, rate values were not used as a measure of acceleration of [^{3}H]spiperone dissociation. This was because data at high modulator concentrations fit to functions that assume two rates of dissociation, whereas data for low concentrations and controls, from short time course experiments (60–80 min), were described by monoexponential functions. The allosteric effect was quantified as the specific [^{3}H]spiperone bound after 20-min radioligand dissociation in the presence of modulator divided by the value obtained for the control. The dependence of this value on the logarithm of the modulator concentration (X) was fit to the equation

$$\%\ \text{Bound}/\%\ \text{bound}_{(\text{control})}\ \text{at 20 min} = A + \frac{1 - A}{1 + (10^B/10^X)^n} \quad (1)$$

where A is the lower plateau of the curve, B is the log(EC_{50}), and n represents the Hill coefficient.

Data from experiments measuring the effect of MIA on [^{3}H]spiperone dissociation, in the presence of amiloride, were subjected to Schild analysis (21). The dependence of calculated dose ratios on amiloride concentration was fit, using linear regression, to the equation

$$\text{Log(dose ratio)} = \log([\text{amiloride}]) + pA_2 \quad (2)$$

where pA_2 represents the estimate of the amiloride affinity. This analysis was also used for the effects of haloperidol and MIA on [^{3}H]spiperone saturation analyses. Dose ratios were calculated as the K_d in the presence of haloperidol or MIA divided by the K_d in its absence.

Association rate constants (k_1) for [^{3}H]spiperone binding were determined from the observed association rates ($k_{1(obs)}$) obtained from the curve-fitting procedure by using the equation

$$k_1 = \frac{k_{1(obs)} - k_{-1}}{[L]} \quad (3)$$

where k_{-1} is the appropriate dissociation rate constant, and [L] is the free [^{3}H]spiperone concentration.

Pseudocompetition and saturation data for [^{3}H]spiperone binding were also analyzed using the binding models outlined in Appendix. SigmaPlot (Jandel Scientific, San Rafael, CA) was used for these analyses.

Statistical significance of differences between data was determined using Student's t tests. EC_{50} values were first converted to the respective normally distributed negative logarithm.

Results

Dissociation of [^{3}H]spiperone from Ltk59 membranes: effects of allosteric modulators. The kinetics of the dissociation of [^{3}H]spiperone from D_2 dopamine receptors were determined after the addition of an excess of the competing ligand (+)-butaclamol. In initial experiments, the dissociation of [^{3}H]spiperone was followed over a 60-min time course, and the data obtained under these conditions were fit to monoexponential functions (Fig. 1), with a mean off-rate of 0.00986 ± 0.00098 min^{-1} (mean ± standard error, seven experiments).

The dissociation of [^{3}H]spiperone was measured in the presence of different concentrations of amiloride during a 60-min time course. Amiloride increased the dissociation rate for [^{3}H]spiperone in a concentration-dependent manner (Figs. 1 and 2), and radioligand dissociation in the presence of all amiloride concentrations was described best by mono-

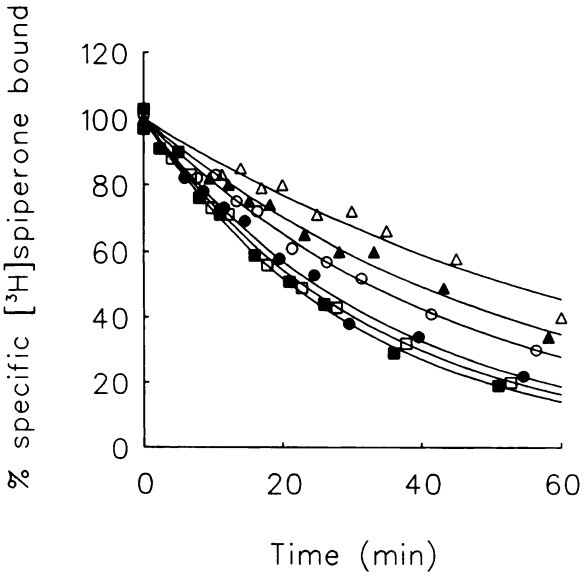

Fig. 1. [^{3}H]Spiperone dissociation from the D_2 dopamine receptor in the presence of amiloride. Dissociation of [^{3}H]spiperone from Ltk59 membranes was measured as described in Experimental Procedures in the absence of modulator (△) and in the presence of a range of amiloride concentrations (▲, 50 μM; ○, 150 μM; ●, 300 μM; □, 750 μM; ■, 1 mM). *Data points*, expressed as the percentage of [^{3}H]spiperone binding in the absence of (+)-butaclamol, after equilibration; *curves*, computer-generated single exponential best fits derived by nonlinear regression analysis of the data points. The data are from a single experiment that was repeated twice with similar results.

exponential functions. The EC_{50} value for the increase of this rate was 347 ± 119 μM (mean ± standard error, three experiments). When measured over longer time courses (≥100 min), dissociation data in the presence of 1 and 3.2 mM amiloride were better fit ($p < 0.01$) by assuming two dissociation rates (data not shown).

The effect of analogs of amiloride on the dissociation of [^{3}H]spiperone was measured over 100 min to examine whether the analogs had effects on the more complex kinetic behavior described above. Monoexponential functions described [^{3}H]spiperone dissociation in the presence of lower analog concentrations (Fig. 3A), but at higher concentrations of amiloride analogs (≥31.6 μM for DMA and benzamil; ≥10 μM for EIA and MIA, and ≥3.2 μM for HMA), analysis of dissociation data was significantly improved ($p < 0.05$) by assuming that there were two off-rates (Fig. 3A). Extension of the time course to 300 min revealed biexponential dissociation for experiments with 1 and 3.2 μM MIA (Fig. 3B) as well as in the absence of the modulators (see below for complete data).

To obtain a measure of the differential effects of the different compounds on dissociation rates, the amount of [^{3}H]spiperone remaining bound after 20 min was determined for different concentrations of the compounds. All of the analogs accelerated [^{3}H]spiperone dissociation with a higher potency than the parent compound (Fig. 2 and Table 1), with a rank order of potency of HMA > MIA > EIA > benzamil > DMA > amiloride. The analogs also produced a greater maximal effect than amiloride, in terms of both the binding remaining after 20-min dissociation (Fig. 2) and the acceleration of the rapid off-rate produced by a saturating modulator concentration (Table 1).

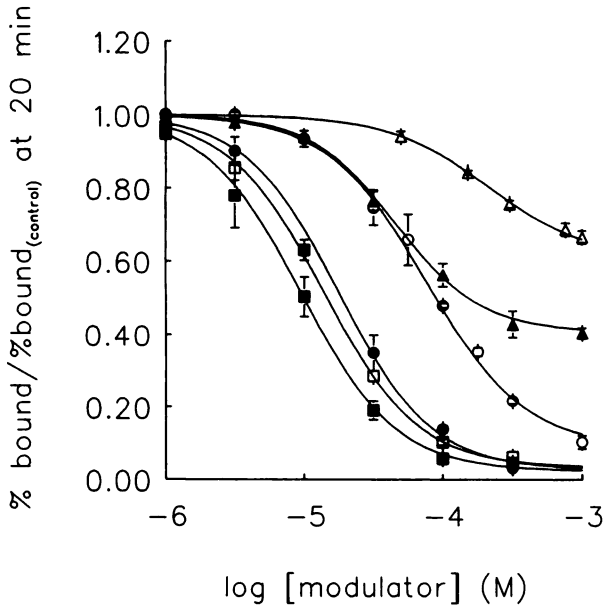

Fig. 2. Concentration dependence of amiloride and amiloride analogs for acceleration of [^{3}H]spiperone dissociation from the D_2 dopamine receptor (△, amiloride; ▲, benzamil; ○, DMA; ●, EIA; □, MIA; ■, HMA). Radioligand dissociation experiments using Ltk59 membranes were carried out as outlined in Experimental Procedures. Acceleration of [^{3}H]spiperone dissociation was quantified as the amount of binding remaining after 20 min of the dissociation phase and expressed as a percentage of this value for dissociation in the presence of the vehicle. The binding at 20 min was calculated from dissociation curves derived by nonlinear regression of the time course data. The concentration dependence of these values was fit to eq. 1. *Data points*, mean ± standard error from three or four experiments; *curves*, defined by eq. 1 using parameters that are averaged from fits to data from three or four experiments.

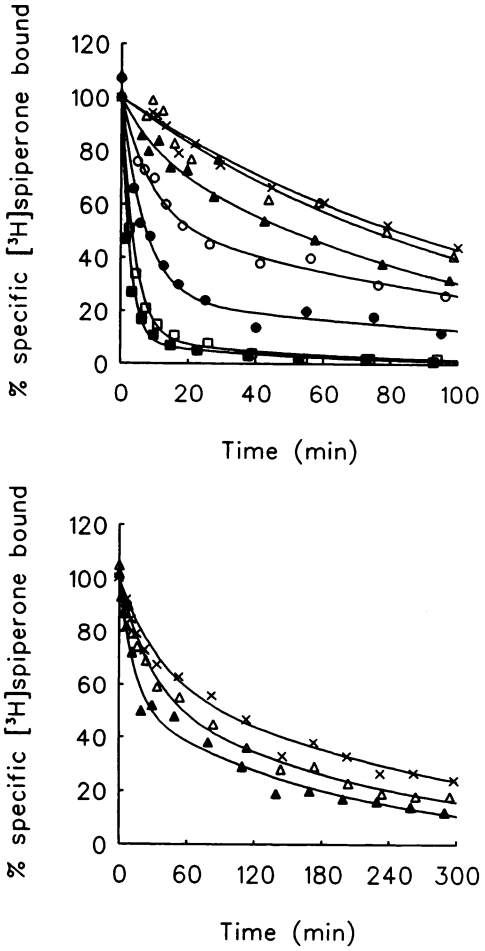

Fig. 3. Dissociation of [^{3}H]spiperone from the D_2 dopamine receptor in the presence of MIA and 0.75% DMSO. The time course of dissociation of [^{3}H]spiperone binding from Ltk59 membranes was performed as described in Experimental Procedures. *Top*, Measurement of [^{3}H]spiperone dissociation for 100 min. Data in the presence of 0.75% DMSO (×), 1 μM MIA (△), and 3.16 μM MIA (▲) are described by monoexponential curves. Biexponential curves improve the goodness of fit ($p < 0.05$) for radioligand dissociation in the presence of 10μM (○), 31.6μM (●), 100μM (□), and 316μM (■) MIA. Data are from a single experiment that was repeated three times. *Bottom*, Five-hour time course of [^{3}H]spiperone dissociation. Extension of the time course reveals the biphasic nature of radioligand dissociation in the presence of 0.75% DMSO (×), 1 μM MIA (△), and 3.16 μM MIA (▲). *Curves* are all biexponential functions, which represent better fits to the data ($p < 0.05$) compared with single-rate functions.

Analysis of [^{3}H]spiperone dissociation over longer time periods: effect of MIA on the kinetics of [^{3}H]spiperone dissociation. Extension of the time course of dissociation to 5 hr revealed biexponential dissociation even in the absence of allosteric modulators; the fit was significantly improved ($p < 0.01$) by assuming two rates of dissociation (Fig. 4B and Table 2). In the experiments described below on the effects of amiloride analogs, DMSO was included as a solvent. When measured over 5 hr (Fig. 3B), analysis of radioligand dissociation in the presence of 0.75% DMSO was significantly improved by using a biexponential function, but the mean kinetic parameters from three experiments [$k_{-1(fast)}$ = 0.0281 ± 0.0077 min^{-1} (39.6 ± 2.8% of specific binding); $k_{-1(slow)}$ = 0.00272 ± 0.00039 min^{-1}] (mean ± standard error, four experiments) were not significantly different ($p > 0.05$) from the corresponding values in the absence of solvent (Table 2).

The addition of MIA accelerated both the slow and rapid rates of [^{3}H]spiperone dissociation (Fig. 5A). Different concentrations of MIA were tested, and dose-response curves were obtained for the effects on the slow and rapid rates. Both response curves closely approximated mass action curves, with the slopes not differing significantly from unity ($p > 0.05$). The EC_{50} values for the acceleration of the two rates (49.7 ± 5.8 μM for $k_{-1(fast)}$ and 42.2 ± 7.1 μM for $k_{-1(slow)}$, mean ± standard error, four experiments) are not significantly different ($p > 0.05$). MIA induced a 14.7 ± 0.8-fold increase of the fast [^{3}H]spiperone dissociation rate. The maximal acceleration of the slow rate (16.1 ± 1.2-fold) was not significantly different ($p > 0.05$) from that of the fast rate.

MIA also modulated the proportion of total [^{3}H]spiperone binding that dissociated at the rapid rate, defined as $P_{(fast)}$ (Fig. 5B). This effect is not described by a mass action curve; a steep slope of 2.26 ± 0.35 (mean ± standard error, four experiments) was obtained from the curve-fitting analysis. The EC_{50} value for this effect was 30.1 ± 1.7 μM, with MIA inducing a maximum $P_{(fast)}$ value of 89.0 ± 1.3%.

Effect of amiloride on acceleration of [^{3}H]spiperone dissociation produced by MIA. Amiloride produces a lower maximal increase of the radioligand dissociation rate compared with MIA (Table 1). This difference was exploited to investigate whether the two modulators act at a common site to produce this effect. The addition of amiloride resulted

TABLE 1

Structure-activity relationship data for amiloride and amiloride analogs for acceleration of [^{3}H]spiperone dissociation from the D_2 dopamine receptor

The time course of radioligand dissociation from Ltk59 membranes was determined as outlined in Experimental Procedures. Data were fit to monoexponential and biexponential functions. The kinetic parameters generated were used to calculate the percentage of specific binding remaining after 20 min, which was then divided by the equivalent value in the presence of the appropriate vehicle. The normalized data were fit to eq. 1 using nonlinear regression to obtain estimates of relative potency (EC_{50}). To obtain a measure of the relative maximal effect of these compounds (E_{max}), the fast dissociation rate at saturating concentrations was divided by the fast [^{3}H]spiperone off-rate for the appropriate vehicle. Time course data in the presence of saturating modulator concentrations are described by two-rate functions. The modulator concentrations in these experiments were amiloride, 3.16 mM; benzamil and DMA, 1 mM; and EIA, MIA, and HMA, 316 μM. Values are mean ± standard error for three or four experiments.

Modulator		EC_{50}	Maximal-fold increase of off-rate
		μM	
Amiloride	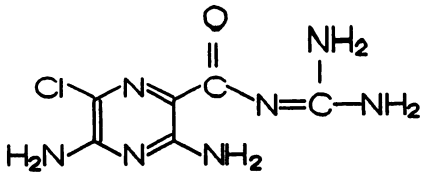	214.8 ± 34.8	2.7 ± 0.2
DMA	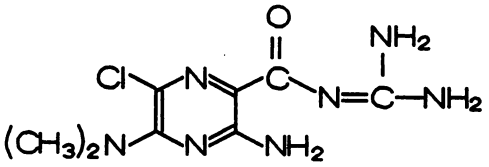	75.5 ± 8.2	8.4 ± 0.9
Benzamil	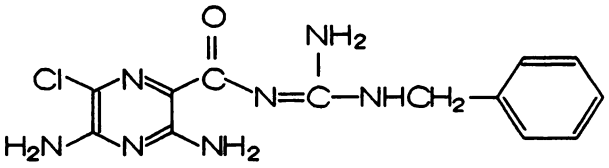	45.5 ± 4.0	4.8 ± 0.7
EIA	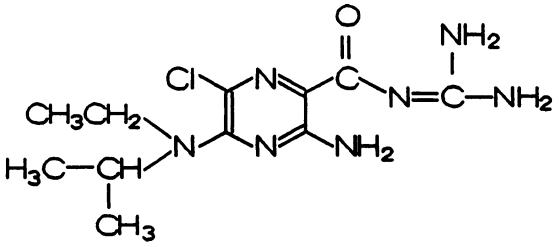	20.2 ± 4.6	17.6 ± 1.5
MIA	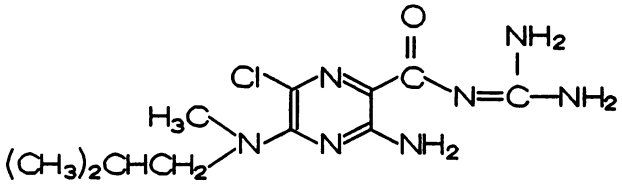	13.8 ± 1.0	14.3 ± 1.8
HMA	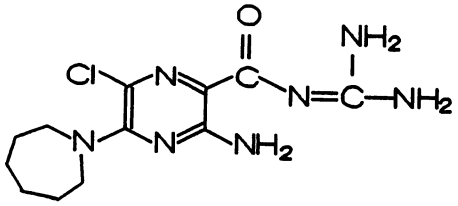	9.5 ± 1.6	16.4 ± 2.8

in a concentration-dependent rightward shift of the MIA response curve (Fig. 6A). The concentration-response curves for the presence and absence of amiloride seemed to be parallel. Analysis of this shift was complicated by the limited solubility of MIA; in the presence of amiloride, it was not possible to obtain a measurement of the maximum response (Fig. 6A). This prevents the calculation of EC_{50} values, which are normally used to calculate dose ratios for Schild analysis (21).

To calculate dose-ratio values, equieffective doses of MIA in the presence of the various amiloride concentrations were determined. This was done for two response values, repre-

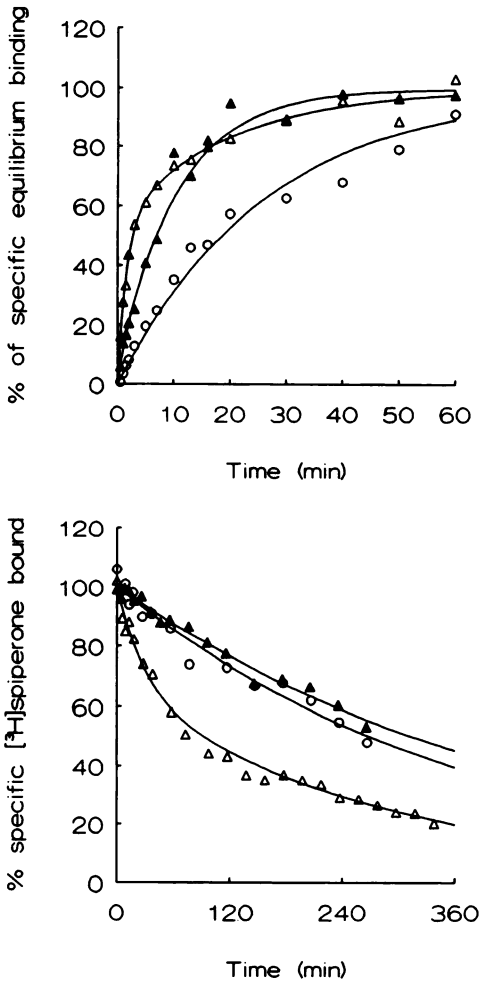

Fig. 4. [^{3}H]Spiperone binding kinetics at the D_2 dopamine receptor with the addition of 6 mM $MgCl_2$ (▲), 6 mM $MgCl_2$, and 100 μM GTP (○) and in the absence of either modulator (△) (the presence of 1 mM EDTA and 1 mM EGTA in the assay buffer results in an effective Mg^{2+} concentration of 4 mM). The experiments were performed as described in Experimental Procedures. *Top*, [^{3}H]Spiperone association to Ltk59 membranes. The data are from representative experiments. Association in the presence of Mg^{2+} and GTP was best described by monoexponential functions, whereas association in the absence of modulators was best described by biexponential functions. The data in the presence of $MgCl_2$ are best described by a biexponential association function in which the fast rate represented 5% of total equilibrium binding. The assay was repeated twice with similar results for the control and in the presence of $MgCl_2$ and GTP and eight times in the presence of $MgCl_2$ (see text for details of these fits). *Bottom*, [^{3}H]Spiperone dissociation from Ltk59 membranes. Data are from a representative experiment that was repeated twice for the control, six times in the presence of $MgCl_2$, and four times in the presence of $MgCl_2$ and GTP with similar results. The curves are monoexponential fits to the $MgCl_2$ and $MgCl_2$/GTP data and biexponential fits to the control data.

sented by [^{3}H]spiperone dissociation rates of 0.125 and 0.175 min^{-1} (Fig. 6A). Schild analysis yields linear plots (Fig. 6B). The slopes obtained at [^{3}H]spiperone dissociation rates of 0.125 and 0.175 min^{-1} were 0.99 ± 0.15 and 0.83 ± 0.10, respectively (mean ± standard error from analysis of pooled dose-ratio data). Neither of these values is significantly different from unity ($p > 0.05$). The estimates of pA_2 were 479 and 339 μM, respectively. Both of these values are close to the EC_{50} value of amiloride when used alone (347 μM).

Analysis of [^{3}H]spiperone association to Ltk59 membranes. The time course of [^{3}H]spiperone association to the D_2 dopamine receptor was described statistically better ($p < 0.05$) by biexponential association curves than by single-rate functions (Fig. 4A and Table 3), and from these fits, two observed association rates can be obtained: $k_{1(obs)slow}$ and $k_{1(obs)fast}$. If these observed association rates are combined with the corresponding values for the slow and fast dissociation rate constants, then association rate constants k_{1slow} and k_{1fast} can be calculated using eq. 3 (Table 3). The association and dissociation rate constants can then be used to obtain values for equilibrium dissociation constants (K_d) = 11.6 and 7.8 pM for the slow and fast components, respectively).

The kinetics of [^{3}H]spiperone binding in the presence of $MgCl_2$ and GTP. Dissociation of [^{3}H]spiperone in the presence of Mg^{2+} was fit best to a single-rate function (Fig. 4B and Table 2). (For these experiments, 6 mM $MgCl_2$ was present in the equilibration and dissociation phases.) The mean dissociation rate was not significantly different ($p > 0.05$) from the slow rate in the absence of modulators (Table 2). In four of nine experiments, [^{3}H]spiperone association in the presence of Mg^{2+} was best described by a single association rate that was similar to the slow rate in the absence of the cation. In the other five experiments, a small proportion of the equilibrium binding was detectable that associated at a more rapid rate; the biexponential fit was a significant improvement ($p < 0.05$) over the single-rate fit. The mean calculated $k_{1(fast)}$ and $k_{1(slow)}$ values (Table 3) were not significantly different from the control rate constants ($p > 0.05$). The proportion of binding associating at the rapid rate (Table 3) was significantly lower ($p < 0.05$) than that of the control. The apparent loss of the faster rates of dissociation and association in the presence of Mg^{2+} suggests that the combination of rates used in Table 3 is correct.

Dissociation of [^{3}H]spiperone in the presence of GTP (100 μM) and Mg^{2+} (6 mM) was best described by monoexponential functions, with the biexponential functions providing no improvement ($p > 0.05$). The dissociation rate measured in these experiments was not significantly different from the value obtained in the presence of Mg^{2+} alone (Table 2; $p > 0.05$). Association of [^{3}H]spiperone in the presence of GTP and Mg^{2+} was best described by a single association rate in all cases (Table 3). The calculated association rate constant was half of that for the absence of GTP (Table 3), but this effect was not statistically significant ($p > 0.05$).

Association of [^{3}H]spiperone to Ltk59 membranes in the presence of 120 mM NaCl or 120 mM NMDG. Association of [^{3}H]spiperone was measured in the presence of 120 mM NMDG to determine whether ionic strength affected the process. Association under these conditions was better described using a biexponential function ($p < 0.05$) than with a single-rate fit (Fig. 7 and Table 4). The observed slow and fast association rates (Table 4) were not significantly different ($p > 0.05$) from the equivalent rates for the control (Table 3). The range of free radioligand concentrations in the presence of NMDG was similar to that in control experiments (239–374 and 217–304 pM, respectively), so the observed association rates are comparable. The presence of NMDG did not significantly affect ($p > 0.05$) the distribution of equilibrium binding that associated at the slow and fast rates (Tables 3 and 4). The presence of 120 mM NMDG accelerated [^{3}H]spiperone dissociation (data not shown). Because of this effect of ionic strength, the effect of NaCl on radioligand dissociation was not tested.

TABLE 2

Kinetic parameters for [^{3}H]spiperone dissociation from the D_2 dopamine receptor: effects of $MgCl_2$ and GTP

Radioligand dissociation from Ltk59 membranes was performed as described in Experimental Procedures. The presence of 1 mM EDTA and 1 mM EGTA results in an effective Mg^{2+} concentration of 4 mM. Parameters are derived from biexponential fits to the data for the control and monoexponential fits for dissociation for the other two experimental conditions. $P_{(slow)}$ and $P_{(fast)}$ represent the fraction of [^{3}H]spiperone binding that dissociates at the slow and fast rate, respectively. Values are mean ± standard error (three experiments for the control, seven experiments for 6 mM $MgCl_2$, and five experiments for $MgCl_2$ and GTP).

Experiment	$k_{-1(slow)}$	$P_{(slow)}$	$k_{-1(fast)}$	$P_{(fast)}$
	min^{-1} (×100)	%	min^{-1} (×100)	%
Control	0.269 ± 0.036	58.2 ± 5.1	2.23 ± 0.61	41.8 ± 5.1
$MgCl_2$	0.305 ± 0.043	100		
$MgCl_2$ + GTP	0.319 ± 0.038	100		

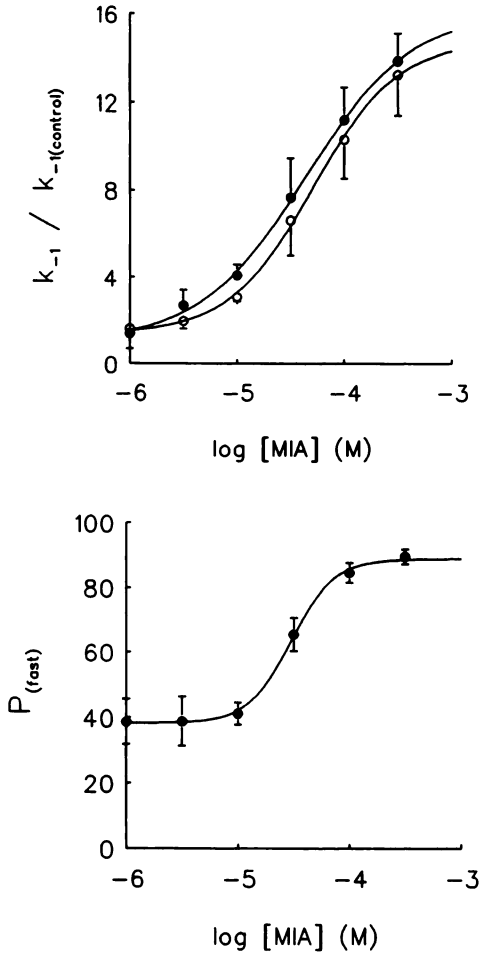

Fig. 5. Effect of MIA on kinetic parameters of [^{3}H]spiperone dissociation from the D_2 dopamine receptor. Biexponential dissociation functions fit to time course data generated four parameters: the slow and fast dissociation rate values and the fractions of total specific binding that dissociate at the slow and fast rates. Data represent the mean ± standard error from four experiments. *Top*, MIA concentration dependence of acceleration of slow (●) and fast (○) dissociation. The slow and fast rates in the presence of different concentrations of MIA were divided by slow and fast dissociation rates, respectively, for [^{3}H]spiperone in the presence of 0.75% DMSO. Curves were generated using a four-parameter logistic equation for each experiment. The curves in the figure are defined by this equation using the mean parameters from the four experiments. *Bottom*, Concentration dependence of MIA for increasing the proportion of [^{3}H]spiperone binding that dissociates at the fast rate ($P_{(fast)}$). The curve is defined by a four-parameter logistic equation using mean parameter values obtained from curve fitting to the four individual experiments.

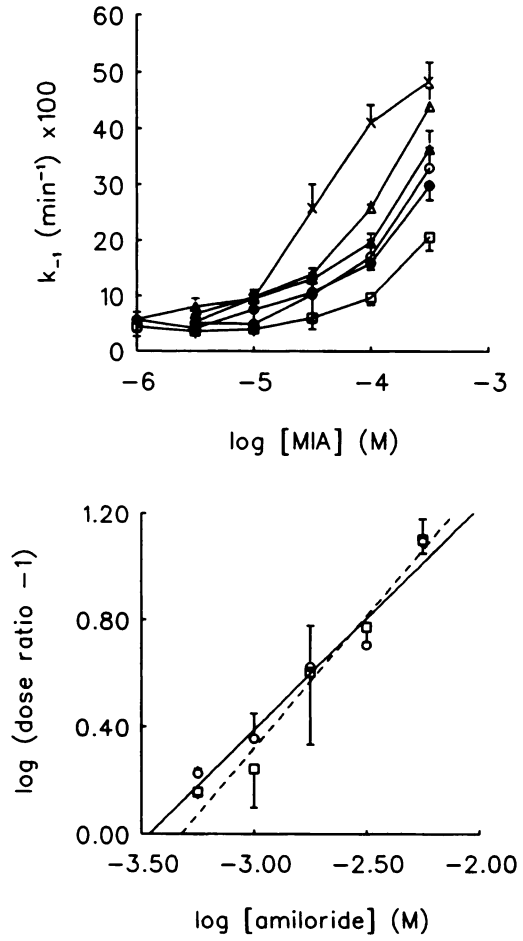

Fig. 6. Acceleration of [^{3}H]spiperone dissociation from the D_2 dopamine receptor produced by MIA in the presence of amiloride. *Top*, MIA concentration-dependence isotherms for increasing the [^{3}H]spiperone off-rate in the presence of a range of concentrations of amiloride (△, 0.56 mM; ▲, 1 mM; ○, 1.78 mM; ●, 3.16 mM; □, 5.62 mM; ×, MIA alone). Radioligand dissociation from Ltk59 membranes was performed as outlined in Experimental Procedures. Dissociation rate values are the rapid rates from biexponential fits to the time course data, which were significantly better ($p < 0.05$) than single-rate fits. *Data points*, mean ± standard error (three or four experiments) or mean ± range (two experiments). *Bottom*, Schild plot of data from *top*. Dose ratios were calculated for two response values, represented by [^{3}H]spiperone rates of 0.125 min^{-1} (□) and 0.175 min^{-1} (○). *Lines*, linear-regression fits of the data to eq. 2 (*dashed line*, 0.125 min^{-1} response value; *solid line*, 0.175 min^{-1} response value). *Data points*, mean ± standard error (three or four experiments) or mean ± range (two experiments).

In the presence of 120 mM NaCl, the slow rate of [^{3}H]spiperone association could not be detected in three experiments; the time course data were fit best by a monoexponential function. In two other experiments, radioligand association was better described ($p < 0.05$) by a two-rate function (Fig. 7 and Table 4). The mean $k_{1obs(fast)}$ value was not significantly different from the mean value obtained in the presence of

TABLE 3

Kinetic parameters for [^{3}H]spiperone association to the D_2 dopamine receptor in the presence and absence of 6 mM $MgCl_2$ and 100 μM GTP

The assays for radioligand association to Ltk59 membranes were carried out as described in Experimental Procedures. Parameters are derived from biexponential fits for the control and monoexponential fits to data in the presence of $MgCl_2$ and GTP, and values are mean ± standard error from three experiments. Data from four experiments performed in the presence of Mg^{2+} alone were statistically better described by monoexponential functions ($p < 0.05$), whereas biexponential functions represented a significant improvement ($p < 0.05$) in five experiments. The slow rate data are mean ± standard error from nine experiments, assuming that the single rate from the monoexponential fits represents the slow rate. The fast rate data are mean ± standard error from the five experiments in which this component was detected. The $P_{(slow)}$ and $P_{(fast)}$ values represent the fractions of total specific [^{3}H]spiperone binding at equilibrium that associate at these slow and fast rates, respectively. The values are mean ± standard error from nine experiments in the presence of $MgCl_2$ where $P_{(slow)}$ was taken as 100% for the monoexponential fits. Association rate constants [$k_{1(slow)}$ and $k_{1(fast)}$] were calculated using eq. 3. It was assumed that the slow on-rate was associated with the slow off-rate, with a similar combination for the fast kinetics, when making these calculations. To calculate $k_{1(fast)}$ in the presence of $MgCl_2$, the fast rate of dissociation in the absence of modulators was used (Table 2).

Experiment	$k_{1obs(slow)}$	$P_{(slow)}$	$k_{1obs(fast)}$	$P_{(fast)}$	$k_{1(slow)}$	$k_{1(fast)}$
	min^{-1}	%	min^{-1}	%	min^{-1} M^{-1} ($\times 10^{-8}$)	min^{-1} M^{-1} ($\times 10^{-9}$)
Control	0.0623 ± 0.0118	53.3 ± 5.1	0.768 ± 0.198	46.7 ± 5.1	2.32 ± 0.22	2.87 ± 0.49
$MgCl_2$	0.0703 ± 0.0164	87.1 ± 4.8	0.482 ± 0.164	12.9 ± 4.8	2.93 ± 0.73	1.94 ± 0.63
$MgCl_2$ + GTP	0.0365 ± 0.0035	100			1.43 ± 0.14	

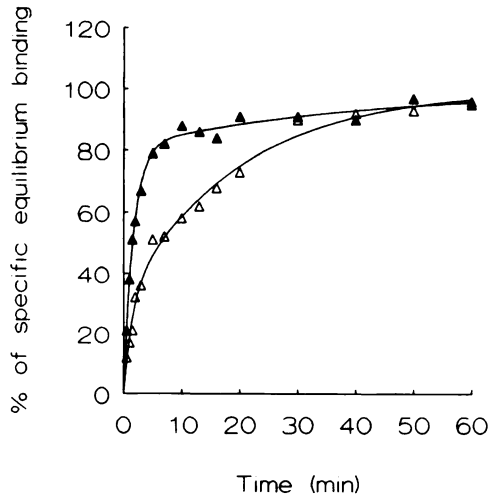

Fig. 7. Association of [^{3}H]spiperone to the D_2 dopamine receptor in the presence of 120 mM NMDG (△) and 120 mM NaCl (▲). The time course of radioligand association to Ltk59 membranes was measured as described in Experimental Procedures. In the presence of NMDG, [^{3}H]spiperone association was described by a biexponential function, which improved the fit compared with a monoexponential function in all cases. In the presence of Na^+, biexponential fits provided an improvement in some cases. Data from the experiment shown were described by a biexponential function. (See legend to Table 4 for details regarding these fits.) Data are from a representative experiment that was repeated four times in the presence of NaCl and twice for the NMDG control.

NMDG (Table 4). The slow observed association rate constant was similar to that observed for NMDG (Table 4). Comparisons of the observed association rates can be made because the free [^{3}H]spiperone concentration was similar in the presence of sodium (213–333 pM) compared with the NMDG experiments (see above). The proportion of equilibrium [^{3}H]spiperone binding that associated at the fast rate was greater in the presence of sodium compared with NMDG (Table 4), and the effect was statistically significant ($p < 0.05$).

Saturation and inhibition analysis of [^{3}H]spiperone binding to Ltk59 membranes: effects of MIA. Equilibrium [^{3}H]spiperone saturation binding experiments were performed under two conditions: large-volume (10 ml) assays to minimize ligand depletion and, more routinely, small-volume (1 ml) assays. Data from these assays were analyzed using a single-site model and a model that assumes two independent sites. For large-volume assays, the single-site analysis provided a good fit to the data in all cases and yielded a K_d value of 16.8 ± 2.5 pM (mean ± standard error six experiments) (Fig. 8). For [^{3}H]spiperone saturation measured using a 1-ml volume, the K_d value was 112 ± 8 pM (mean ± standard error, 45 experiments) for the control and 147 ± 35 pM in the presence of 0.75% DMSO (mean ± standard error, five experiments). The effects of a range of concentrations of haloperidol and MIA on [^{3}H]spiperone saturations was tested using the latter procedure, and the data were analyzed using Schild analysis (Fig. 9). This experiment for haloperidol was performed to determine whether the procedure was suitable for characterizing ligands despite the inaccuracy of K_d determination resulting from ligand depletion (see Experimental Procedures). For haloperidol, the effects were to increase the apparent K_d without affecting B_{max} (Fig. 9), and Schild analysis of the data was consistent with a competitive interaction at the receptor (Schild slope = 1.05 ± 0.11, mean ± standard error from pooled dose-ratio data; pA_2 = 8.40). For MIA, the apparent K_d increased and B_{max} was not significantly affected except at the highest concentration of MIA (Fig. 9). Schild analysis of the data excluding the value at the highest MIA concentration indicated a noncompetitive interaction. Schild analysis yielded a slope of 1.43 ± 0.16 (mean ± standard error from analysis of pooled dose-ratio data). This mean slope value is significantly different from unity ($p < 0.05$). The pA_2 value was 5.28 (equivalent to 5.25 μM).

MIA was also tested in inhibition experiments versus a single concentration of [^{3}H]spiperone (Fig. 10 and Appendix) (pseudocompetition experiment). MIA inhibited all specific [^{3}H]spiperone binding, and the Hill slope of the inhibition curve was 2.15 ± 0.06 (mean ± standard error, three experiments). These data and data from the saturation analyses were analyzed using various models for the interactions of ligands at allosteric and competitive sites; details are given in the Appendix.

Discussion

The allosteric regulation of D_2 dopamine receptors by amiloride and amiloride analogs is described. The effects of this allosteric modulation have been examined in kinetic and equilibrium experiments, and models for the regulation are proposed.

TABLE 4

Kinetic parameters for [^{3}H]spiperone association to the D_2 dopamine receptor in the presence of 120 mM NMDG or 120 mM NaCl

Association of [^{3}H]spiperone to Ltk59 membranes was measured as outlined in Experimental Procedures. Biexponential functions described the time course of radioligand association in the presence of NMDG, and the parameters are mean ± standard error from three experiments. Data from three experiments performed in the presence of NaCl were better described ($p > 0.05$) by monoexponential functions, whereas a two-rate fit improved the analysis ($p < 0.05$) in two additional experiments. The fast rate data are mean ± standard error from all five experiments, whereas the slow rate value is the mean ± range from the two experiments in which this component was detected. The $P_{(slow)}$ and $P_{(fast)}$ values represent the fractions of total specific [^{3}H]spiperone binding that associate at the slow and fast rates, respectively. The values are the mean ± standard error from all five experiments, in which $P_{(fast)}$ was taken as 100% for the monoexponential fits.

Experiment	$k_{1obs(slow)}$	$P_{(slow)}$	$k_{1obs(fast)}$	$P_{(fast)}$
	min^{-1}	%	min^{-1}	%
NMDG	0.0502 ± 0.0019	62.0 ± 3.8	0.499 ± 0.088	38.0 ± 3.8
NaCl	0.0829 ± 0.0580	15.4 ± 11.3	0.500 ± 0.140	84.6 ± 11.3

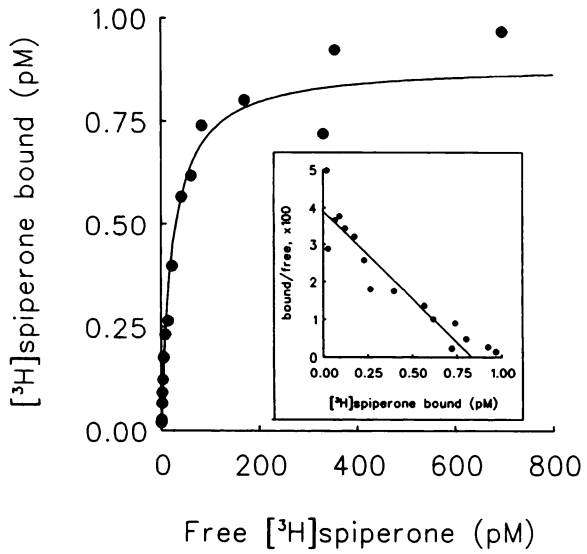

Fig. 8. [^{3}H]Spiperone saturation of the D_2 dopamine receptor measured using a large-volume assay (10 ml). This method, described in Experimental Procedures, permits an accurate determination of K_d of the radioligand. The data are from a single experiment that was repeated five times. The *curve* is defined by a single-site binding isotherm. *Inset*, Scatchard transformation of the data. The *line* is defined by parameters generated by nonlinear regression analysis of the saturation curve using a single-site binding isotherm.

Allosteric regulation by amiloride and amiloride analogs of the binding of [^{3}H]spiperone to D_2 dopamine receptors was first studied through investigation of the ability of these compounds to alter the dissociation kinetics of the radioligand. All of the analogs tested accelerated [^{3}H]spiperone dissociation from the D_2 dopamine receptor with higher potencies than amiloride itself and gave greater maximal accelerations of dissociation (Fig. 2 and Table 1). Two structural classes of amiloride analogs, commonly used for structure-activity determinations on amiloride-binding proteins, were included in this study. These were analogs substituted at the 5-amino group of the pyrazine ring and a terminal guanidino-nitrogen-substituted derivative, benzamil. In common with modulation of the Na^+/H^+ exchanger and the L-type calcium channel, hydrocarbon substituents at the 5-pyrazinoyl-nitrogen increased potency, with the EC_{50} value decreasing with increasing hydrocarbon chain length (22, 23).

In contrast to modulation of Na^+/H^+ exchange, the terminal guanidino-substituted derivative benzamil accelerated radioligand dissociation with a higher potency than the parent compound (22). This suggests that allosteric regulation of the D_2 dopamine receptor is not a reflection of the ability of the receptor to modulate Na^+/H^+ exchange. A similar finding has been reported for the α_2-adrenergic receptor (24). Compounds of the amiloride series have been used in microphysiometry studies to implicate the Na^+/H^+ exchanger in extracellular acidification responses (25–27). However, compounds of the amiloride series modulate ligand binding to the D_2 dopamine receptor and affect ligand binding at the D_3 and D_4 subtypes (28), so the results of these microphysiometric studies are likely to be difficult to interpret.

The rank order of potency of these amiloride analogs for allosteric modulation of the D_2 receptor is similar to that for regulation of the cardiac L-type calcium channel (23). The EC_{50} values at the D_2 dopamine receptor are, however, 4–12-fold greater than those at the calcium channel (23), and the L cells used for some of the experiments reported here do not have these channels (29), so the effects observed are unlikely to be due to the calcium channel. From the current data, it is not possible to assign the site of action of the modulators, but based on data for the α_2-adrenergic receptor (14), it seems likely that modulation of the rate of [^{3}H]spiperone dissociation is a result of an interaction with an allosteric site on the receptor itself.

It has been proposed that allosteric modulation by hydrophobic compounds could be due to nonspecific disruption of the lipid environment (30). Therefore, it was important to determine whether the compounds used in the current study acted at a specific site. The difference in the maximal acceleration of [^{3}H]spiperone dissociation produced by amiloride, compared with MIA (Fig. 2 and Table 1), was exploited to test the nature of the allosteric interaction. [This difference was used in a study on the M_2 muscarinic acetylcholine receptor to demonstrate a competitive interaction between two allosteric modulators (31).] In the current study, amiloride inhibited the effect of MIA, resulting in a parallel rightward shift of the MIA response curve (Fig. 6A). This observation cannot be accounted for by a nonspecific membrane effect and indeed suggests that the modulators are acting at a specific site on the receptors.

Linear Schild plots (Fig. 6B), together with Schild slopes that did not differ significantly from unity, are consistent with a model that assumes that amiloride competes with MIA for a common site. The pK_b value was close to that obtained for amiloride alone. This estimate did not take into account the small effect of amiloride itself on the increase in the dissociation rate. By analogy with Schild analysis of the effect of partial agonists, this activity can be taken into account using the equation

$$K_{b(observed)} = K_b(1-\alpha_p)^{-1} \quad (4)$$

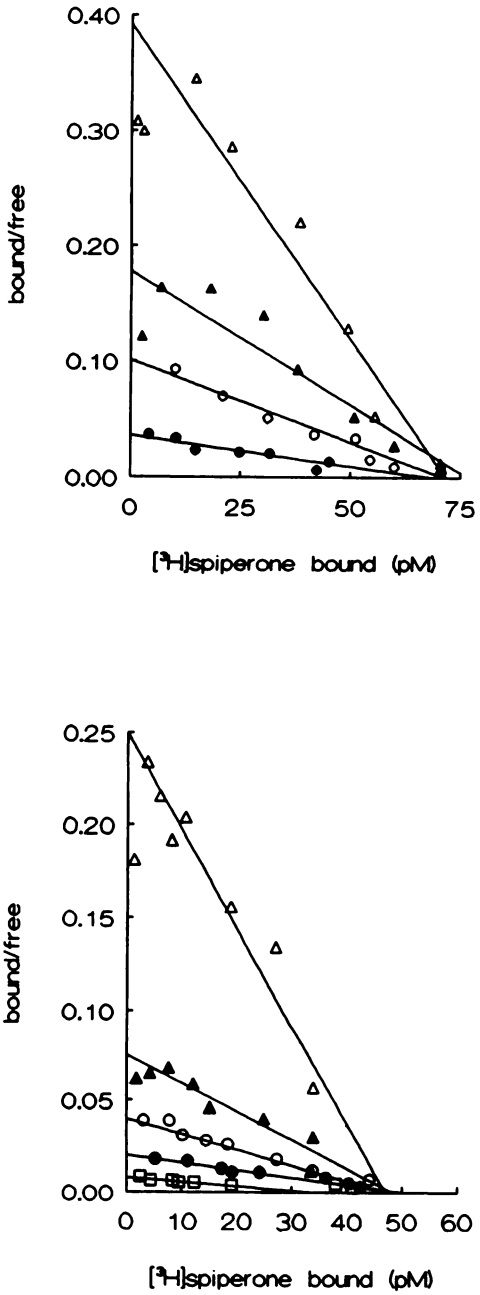

Fig. 9. [^{3}H]Spiperone saturation of the D_2 dopamine receptor showing the effects of haloperidol and MIA. Equilibrium binding of [^{3}H]spiperone binding to Ltk59 membranes was performed as described in Experimental Procedures using an assay volume of 1 ml. *Top*, Scatchard plots of saturation data for [^{3}H]spiperone alone (△) and in the presence of haloperidol (▲, 10 nM; ○, 32 nM; ●, 100 nM). *Bottom*, Scatchard plots of saturation data for [^{3}H]spiperone in the presence of 0.75% DMSO (△) and in the presence of MIA (▲, 10 μM; ○, 14.8 μM; ●, 21.4 μM; □, 31.6 μM). *Lines* are defined by parameters generated by nonlinear regression analysis of saturation curves, and the experiments have been repeated two more times with similar results. Lower concentrations of MIA were also tested in other experiments. Data for all MIA concentrations are presented in Fig. 11.

where α_p is the maximal response of the partial effector expressed as a fraction of the maximal response of the "Full" effector (32). This correction would be needed if the maximal effect was an appreciable fraction of that produced by the "Full" effector: in this study, the value was small (~12%), which slightly reduced the K_b. The use of Schild analysis, as applied here, provides a means for demonstrating competitive interaction of allosteric modulators at the same allosteric site.

In extended dissociation experiments, [^{3}H]spiperone was seen to dissociate at two rates even in the absence of modulators, and it was necessary to perform these longer experiments to reveal this behavior. MIA produced a complex modulation of these two rates of [^{3}H]spiperone dissociation from the D_2 dopamine receptor. The compound increased both the slow and rapid dissociation rates, acting at a similar potency and inducing the same maximal acceleration for the two rates (Fig. 5A). These changes were described by mass action curves. A second effect was the increase of the proportion of [^{3}H]spiperone dissociating at the fast rate ($P_{(fast)}$) (Fig. 5B). The concentration dependence of this effect was described by a steep curve with a Hill coefficient close to 2. This suggests that MIA may be acting at more than one site and that its effects may exhibit a degree of cooperativity. The biphasic nature of dissociation of [^{3}H]spiperone (Figs. 3B and 4B and Table 2) suggests that there are two classes of binding site for the radioligand. Results from [^{3}H]spiperone association experiments are consistent with this idea; the process is again described by two rates (Fig. 4A and Table 3). However, in agreement with a large number of other studies (13, 19, 35, 36), equilibrium binding was well described using a single-site model (9). If it is assumed that the slow association rate is linked with the slow dissociation rate and the rapid kinetic parameters are similarly paired, estimates of K_d by division of k_{-1}/k_1 are very similar (11.6 and 7.8 pM, respectively). The values would be too similar to be reliably distinguished using [^{3}H]spiperone saturation experiments. The dissociation constant determined here in large-volume assays (16.8 pM) is in reasonably good agreement with these estimates. This value is lower than that obtained in other studies (typically, 50–100 pM) (13, 19, 35, 36) and the value obtained using a smaller-assay volume (1 ml) in this study. The membrane protein concentration used in the larger-volume assay (3–4.5 μg/ml) was very low compared with other studies, and this low concentration was used to avoid errors in K_d determination produced by depletion of the lipophilic radioligand (20). The higher K_d values obtained by others and in the smaller-volume assay may be due to this phenomenon (see Refs. 32 and 33 for a more-detailed discussion of this effect). Although the use of the smaller-assay volume does lead to an overestimation of the K_d of the radioligand, this assay design is required for practical reasons in the routine application of ligand-binding assays.

These data on the binding of [^{3}H]spiperone to the recombinant D_2 dopamine receptor suggest that there are two binding sites that can be distinguished kinetically but not in equilibrium binding experiments. The two classes of binding site could correspond to two populations of receptors (see below), and the complex effects of MIA could be a result of effects on these two populations of receptors. Acceleration of the slow and fast dissociation processes may be a result of MIA binding at an allosteric site that is present on both receptor states, with the increased rate resulting from a conformational change in the receptor/ligand complex. This idea is supported by the mass action concentration-dependence curves for the increase in the two rates (Fig. 5A). The similar effects of MIA on the two rates (Fig. 5A) suggest that the modulator binds in a similar manner and elicits a similar

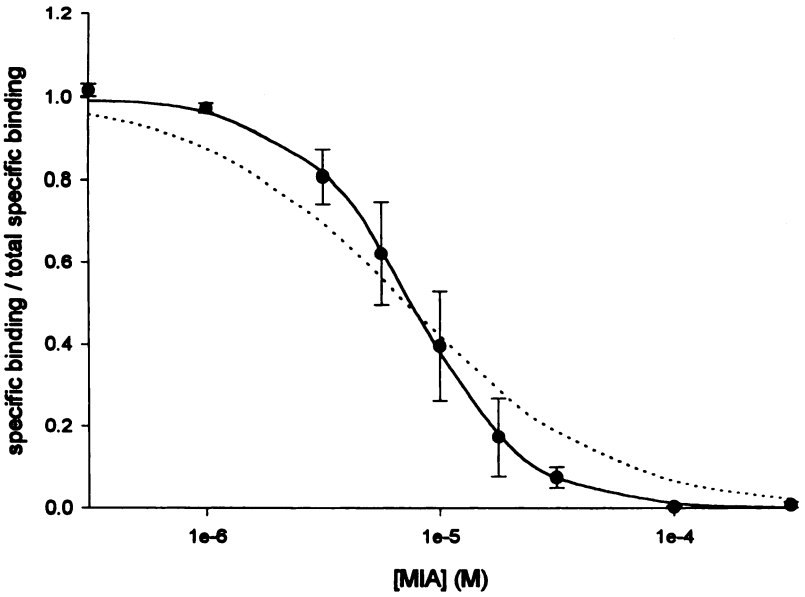

Fig. 10. Curve-fitting analysis of data from [^{3}H]spiperone/MIA pseudocompetition experiments. Data were analyzed in terms of a competitive model (eq. 7) and an allosteric model (eq. 6) (*dashed lines*, which overlie one another). The data were also analyzed using a model that assumes competitive and allosteric modulation of [^{3}H]spiperone binding by MIA (eq. 5) (*solid line*, defined by the following parameter estimates: $\alpha = 0.25$, $\beta = 27.4$, $K_C = 47{,}600\ \text{M}^{-1}$, $K_A = 43{,}200\ \text{M}^{-1}$). The analysis was performed on pooled data from three experiments. The values of K_L and [L] that were used were $6.80 \times 10^9\ \text{M}^{-1}$ and 1.70×10^{-10} M, respectively. *Data points*, mean ± standard error (three experiments). Although these data provide a qualitative comparison of the different models, they were not used to obtain quantitative estimates of the parameters of eq. 1 because of the limited number of data points.

conformational change at both receptor states. The MIA-induced increase of $P_{(fast)}$ (Fig. 5B) suggests that the modulator is also able to alter the distribution of the two putative receptor populations. This effect may be the result of differential binding to another site that could be the receptor binding site. The high slope of the curve suggests that there is a degree of positive cooperativity for this effect.

The nature of the two binding states implied from the kinetic experiments was investigated using Na^+, Mg^{2+}, and GTP. These effectors have been shown to modulate the distribution of receptor states that bind agonist ligands with different affinity (34–36). The ions altered the proportions of the two states without affecting the rate constants for [^{3}H]spiperone binding. The presence of Mg^{2+} shifted the distribution of slow and fast kinetic states in favor of the slow state. Conversely, the effect of Na^+ in association experiments was to alter this distribution in favor of the fast state. The behavior of GTP was tested in the presence of Mg^{2+}, and although there were effects of GTP in some experiments, these were not significantly different from those of Mg^{2+} alone. It seems likely that the states represent two conformationally distinct populations of receptors and that Na^+ and Mg^{2+} act to shift an equilibrium between these states without altering the binding characteristics of each population. The distribution of these two putative populations in [^{3}H]spiperone association experiments is similar to that observed for radioligand dissociation. This suggests that a similar distribution of the binding states is present in the absence of added ligand.

The effects of Mg^{2+}, Na^+, and GTP on the regulation of agonist binding have been interpreted in terms of a ternary complex model in which agonist binding promotes receptor/G protein interaction (35, 37). Receptor/G protein interaction is generally promoted by Mg^{2+} and discouraged by GTP and Na^+. The effects of these modulators on the distribution of the two populations of sites seen here in the kinetic experiments are, therefore, not consistent with these sites resulting from receptor/G protein interaction.

Multiple binding states for [^{3}H]spiperone have been reported for D_2 dopamine receptors of the anterior pituitary (34) and striatum (38). [^{3}H]Spiperone binds at two sites with different affinities in pituitary tissue, and the presence of GTP converts the low affinity state to the high affinity state. A different binding mechanism has been described for striatal dopamine receptors. Equilibrium binding analysis reveals only a single affinity state, but the interaction of [^{3}H]spiperone involves a postbinding isomerization reaction that may involve a further interaction with G proteins. The results for the kinetics of [^{3}H]spiperone binding in this study are different from either of these two investigations. The differing binding mechanisms for [^{3}H]spiperone at the receptor in the three tissues suggest that the cellular environment of the receptor is important for defining regulation. This effect has been demonstrated for α_2-adrenergic receptors (39).

The demonstration of allosteric modulation using kinetic analysis implies regulation of the receptor that should be demonstrable in equilibrium binding experiments. This was indeed the case, and MIA inhibited the binding of [^{3}H]spiperone to D_2 dopamine receptors when included in saturation experiments (Fig. 9). This effect could also be seen when a range of concentrations of MIA were tested against a fixed [^{3}H]spiperone concentration in an inhibition (pseudocompetition) experiment (Fig. 10 and Appendix). The effects of MIA could not be described simply as a competitive interaction at the competitive binding site of the receptor because the Hill coefficient of the pseudocompetition curve was ~2 and because when the effects of MIA in the saturation analyses were subjected to Schild analysis, a Schild slope of >1 was seen. In a corresponding experiment using a range of concentrations of haloperidol, a Schild slope close to 1 was seen, supporting the idea that this compound interacts with [^{3}H]spiperone at the competitive site; thus, competitive interactions can be detected in this manner. Therefore, some of the effects of MIA must be allosteric, as also indicated by the kinetic experiments, but competitive interactions cannot be ruled out. The results of the inhibition and saturation experiments do not allow a clear decision to be made on this point. In the inhibition experiment, a purely allosteric effect would be likely to give only partial inhibition of radioligand binding, but a strongly negatively allosteric effector might give results

TABLE 5

Parameters from curve-fitting analysis of [^{3}H]spiperone saturation of the D_2 dopamine receptor in the presence of MIA

The parameters were obtained from curve-fitting analysis of saturation data presented in Fig. 9 to eq. 5. The analysis was performed for each concentration of MIA (except 31.6 μM for the reasons given in the text) to obtain the estimates of the parameters of the model. Values are mean ± standard error from fits to data from three or four experiments. The value of K_L used in these analyses was the [^{3}H]spiperone association constant obtained in the presence of 0.75% DMSO, which was measured in a vehicle control assay in each experiment. Mean value of parameters are α = 0.45, β = 6.13, K_C = 65,700 M^{-1}, and K_A = 57,900 M^{-1}.

Parameter	MIA concentration				
	4.6	6.8	10	14.8	21.4
			μM		
α	0.74 ± 0.07	0.55 ± 0.01	0.41 ± 0.03	0.30 ± 0.01	0.25 ± 0.07
β	4.92 ± 0.55	5.77 ± 0.17	6.12 ± 0.63	6.44 ± 0.90	7.42 ± 1.08
K_C, M^{-1} ($\times 10^{-4}$)	5.92 ± 0.43	6.32 ± 0.16	6.43 ± 0.63	6.63 ± 0.89	7.54 ± 1.02
K_A, M^{-1} ($\times 10^{-4}$)	5.30 ± 0.56	5.95 ± 0.15	6.05 ± 0.62	6.07 ± 0.94	6.91 ± 1.26

that were difficult to distinguish from complete inhibition (1, 2, 11).

We considered various models in which to describe these observations on the effects of MIA (Appendix) and found that a model that assumes effects of MIA at the allosteric and competitive binding sites of the receptor fits the data well. Negatively cooperative interactions are seen between MIA acting at the allosteric site and [^{3}H]spiperone binding to the competitive binding site, whereas positively cooperative interactions are seen between molecules of MIA binding to the allosteric and competitive sites. According to eq. 5 (see Appendix), the negatively cooperative interaction is signified by values of $\alpha < 1$, and the positively cooperative binding of MIA is signified by values of $\beta > 1$. The effects of haloperidol on [^{3}H]spiperone saturation (Schild slope not significantly different from unity) were consistent with eq. 7 (competitive inhibition), so the more-complicated models were not used to analyze these data. Modulation of antagonist binding to the M_1 muscarinic acetylcholine receptor by tetrahydoaminoacridine is described by an inhibition curve with a steep slope (40). The model described above may also be applicable for this modulatory process.

The question can then be asked of whether the effects of MIA in saturation and inhibition experiments are related to the effects of this modulator on the kinetics of ligand binding. The effects of MIA on saturation and inhibition experiments are on the radioligand-bound and free receptors, whereas the effects on the dissociation kinetics of ligand binding are on the radioligand-bound receptor only. For saturation and inhibition experiments, the models in the Appendix describe the allosteric effect of MIA at the free receptor (defined by K_A) and the radioligand-bound receptor (defined by αK_A). For radioligand dissociation experiments, the effect is quantified for the radioligand-bound receptor (defined by αK_A). K_A and α have been estimated from the analysis of the saturation data described in the Appendix (mean values are from the legend to Table 5), and these give a value for αK_A of 26,055 M^{-1} (38.4 μM expressed as a dissociation constant). This value is in good agreement with EC_{50} values for the increase in the dissociation rate measured above (49.7 and 42.2 μM for the slow and fast rates, respectively), indicating that the effects on equilibrium binding and kinetics may be linked.

We demonstrated allosteric modulation of the D_2 dopamine receptor by amiloride and its analogs based on kinetic and equilibrium experiments. New models have been formulated to describe this allosteric modulation, and insights in to the function of the D_2 dopamine receptor have been obtained. The allosteric site (or sites) identified by these compounds on the D_2 dopamine receptor may provide a new target for ligands that can selectively bind to the different dopamine receptor subtypes.

Acknowledgments

We thank Dr. Sebastian Lazareno for advice and Drs. Derek Middlemiss, Graham Riley, and Martyn Coldwell for interest and support.

Appendix

A general model for the interaction of an allosteric modulator (M) with the competitive and allosteric binding sites of a receptor for a ligand (L) is shown below.

$$\begin{array}{ccccc} LR + M & \overset{K_L}{\rightleftharpoons} & M + L + R & \overset{K_C}{\rightleftharpoons} & L + RM_C \\ \downarrow\uparrow \alpha K_A & & \downarrow\uparrow K_A & & \downarrow\uparrow \beta K_A \\ M_ALR + M & \overset{\alpha K_L}{\rightleftharpoons} & M_AR + L + M & \overset{\beta K_C}{\rightleftharpoons} & L + M_ARM_C \end{array} \quad (5)$$

M_A and M_C denote modulator bound to the allosteric and competitive sites of the receptor, respectively; K_L is the equilibrium association constant for ligand binding to free receptor; K_A is the equilibrium association constant for binding of M to the allosteric site; K_C is the equilibrium association constant for binding of M to the competitive site; and α and β are the cooperativity factors for M (acting at the allosteric site) affecting the binding of L and M, respectively, at the competitive site.

For this general model, the concentration of ligand bound in the presence of M can be expressed as a fraction of that seen in the absence of M ([RL_t]) (Eq. 5). (The following equations were derived using methods outlined in Ref. 12.)

$$\frac{[RL] + [M_ARL]}{[RL_t]} \quad (6a)$$

$$= \frac{(1 + [L]K_L)(1 + \alpha[M]K_A)}{1 + [M]K_C + [L]K_L(1 + \alpha[M]K_A) + [M]K_A(1 + \beta[M]K_C)}$$

Eq. 5 can then be simplified for various submodels of the general model.

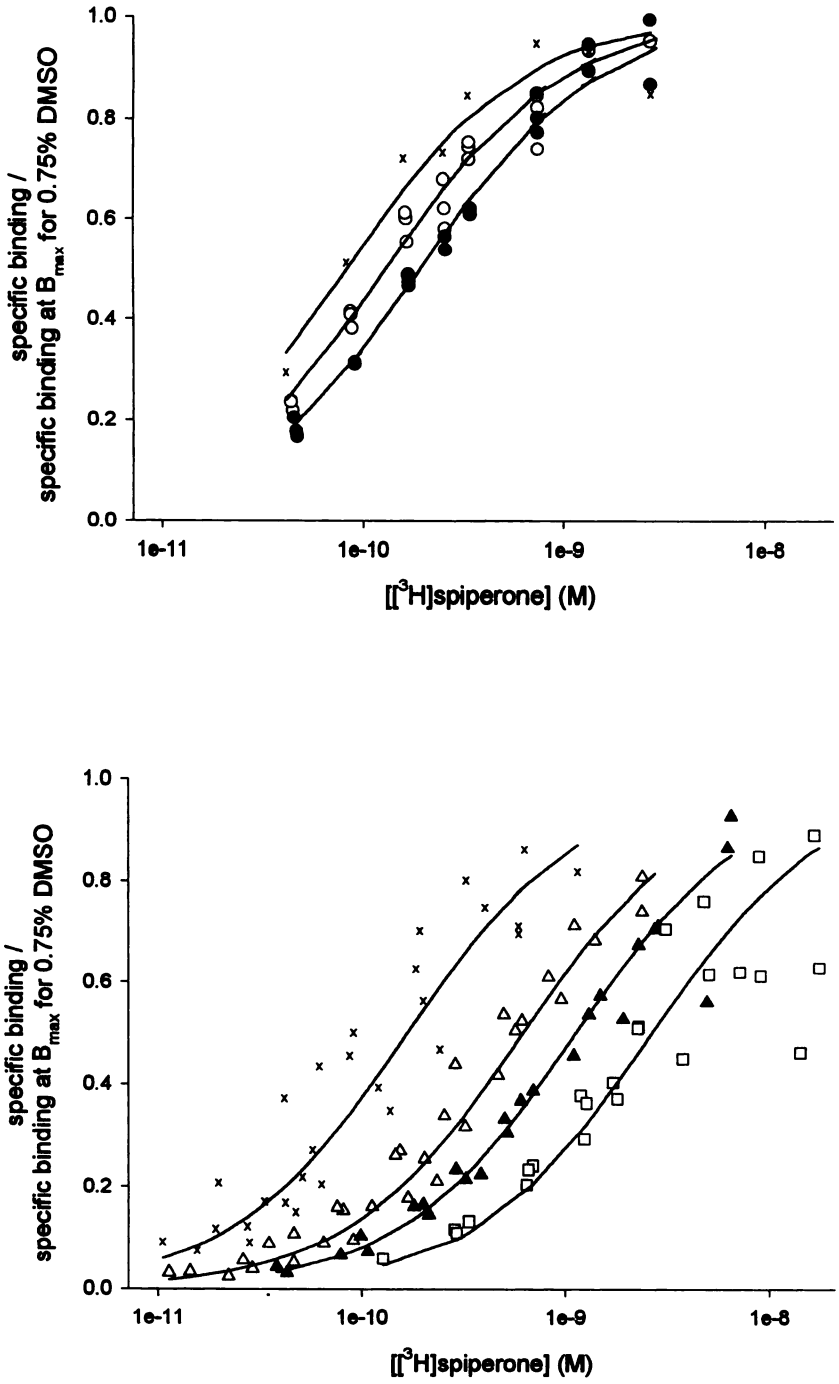

Fig. 11. Saturation data for [^{3}H]spiperone binding in the presence of increasing concentrations of MIA. The data from Fig. 9 have been fit to eq. 5 (×, 0.75% DMSO; ○, 4.6 μM MIA; ●, 6.8 μM MIA; △, 10 μM MIA; ▲, 14.8 μM MIA; □, 21.4 μM MIA). *Curves* for data in the presence of MIA are defined by the mean parameters obtained from the fits to data from the individual experiments (three or four experiments) that are presented in Table 5. Data are the pooled fractional occupancy values from all experiments. *Top*, Effects of 4.6 and 6.8 μM MIA on [^{3}H]spiperone saturation. Three assays at each concentration were performed in a single experiment that included a single vehicle control assay. *Bottom*, Effects of MIA at concentrations of 10, 14.8, and 21.4 μM on [^{3}H]spiperone saturation. One assay for each concentration, together with a vehicle control, was performed in each experiment. This experiment was repeated three times. In an additional experiment, [^{3}H]spiperone saturation in the presence of 10 μM MIA was measured together with saturation for the vehicle control. *Data points* for the vehicle control and 10 μM MIA are from these four experiments.

If M does not bind to the competitive site but only to the allosteric site, then eq. 6 holds:

$$\frac{[RL] + [M_ARL]}{[RL_t]} = \frac{(1 + [L]K_L)(1 + \alpha[M]K_A)}{1 + [M]K_A + [L]K_L(1 + \alpha[M]K_A)} \quad (6b)$$

This equation describes the allosteric model proposed for modulation of muscarinic acetylcholine receptors by gallamine (2).

If M binds only at the competitive site and has no allosteric binding site, then eq. 7 holds:

$$\frac{[RL]}{[RL_t]} = \frac{1 + [L]K_L}{1 + [L]K_L + [M]K_C} \quad (7)$$

The data from Figs. 9 and 10 have been fit to the three models. The goodness of fit of the three equations was compared for the pseudocompetition data (Fig. 10). An F test was performed of the comparison of the residual sum of squares for the different fits according to the "extra sum of squares" principal. The F value was calculated using the following equation: $F = [(SS_1 - SS_2)/(df_1 - df_2)]/(SS_2/df_2)$, where SS_1 and SS_2 represent the residual sum of squares for the fit to the simpler equation (fewer parameters) and more complex equation (more parameters), respectively, and df_1 and df_2 represent the corresponding degrees of freedom for the residuals. The comparison of eq. 6 with eq. 5 yielded $F_{(2,4)} = 85.8$ ($p < 0.001$), and the comparison of eqs. 5 and 7 yielded $F_{(3,4)}$

= 57.1 ($p < 0.001$). These results indicated that eq. 5 provided a significantly better fit to the pseudocompetition data than eqs. 6 and 7. The fits to the saturation data for Fig. 9 are shown in Fig. 11. Mean values of the derived parameters are given in the Table 5, and these imply a negatively cooperative interaction between M and L and a positively cooperative interaction between molecules of M bound at the allosteric and competitive sites.

References

1. Tucek, S., and J. Proska. Allosteric modulation of muscarinic acetylcholine receptors. *Trends. Pharmacol. Sci.* **16**:205–212 (1995).
2. Stockton, J. M., N. J. M. Birdsall, A. S. V. Burgen, and E. C. Hulme. Modification of the binding properties of muscarinic receptors by gallamine. *Mol. Pharmacol.* **23**:551–557 (1983).
3. Ellis, J., M. Seidenberg, and M. R. Brann. Use of chimeric muscarinic receptors to investigate epitopes involved in allosteric interactions. *Mol. Pharmacol.* **44**:583–588 (1993).
4. Matsui, H., S. Lazareno, and N. J. M. Birdsall. Probing of the location of the allosteric site on m1 muscarinic receptors by site-directed mutagenesis. *Mol. Pharmacol.* **47**:88–98 (1995).
5. Lee, N. H., and E. E. El-Fakahany. Allosteric interactions at the m1, m2 and m3 muscarinic receptor subtypes. *J. Pharmacol. Exp. Ther.* **256**:468–479 (1991).
6. Ellis, J., J. Huyler, and M. R. Brann. Allosteric regulation of cloned m1–m5 muscarinic receptor subtypes. *Biochem. Pharmacol.* **42**:1927–1932 (1991).
7. Bruns, R. F., and J. H. Fergus. Allosteric enhancement of adenosine A_1 receptor binding and function by 2-amino-3-benzoylthiophenes. *Mol. Pharmacol.* **38**:939–949 (1990).
8. Bruns, R. F., J. H. Fergus, L. L. Coughenour, G. G. Courtland, T. A. Pugsley, J. H. Dodd, and F. J. Tinney. Structure-activity relationships for enhancement of adenosine A_1 receptor binding by 2-amino-3-benzoylthiophenes. *Mol. Pharmacol.* **38**:950–958 (1990).
9. Mudumbi, R. V., S. C. Montamat, R. F. Bruns, and R. E. Vestal. Cardiac functional responses to adenosine by PD 81,723, an allosteric enhancer of the adenosine A_1 receptor. *Am. J. Physiol.* **264**:H1017–H1022 (1993).
10. Birdsall, N. J. M., E. C. Hulme, W. Kromer, B. S. Peck, J. M. Stockton, and M. J. Zigmond. Two drug binding sites on muscarinic receptors, in *New Concepts in Alzheimer's Disease* (M. Briley, A. Kato, and M. Weber, eds.). Macmillan, London (1986).
11. Ehlert, F. J. Estimation of the affinities of allosteric ligands using radioligand binding and pharmacological null methods. *Mol. Pharmacol.* **33**:187–194 (1988).
12. Lazareno, S., and N. J. M. Birdsall. Detection, quantitation, and verification of allosteric interactions of agents with labeled and unlabeled ligands at G protein-coupled receptors: interactions of strychnine and acetylcholine at muscarinic receptors. *Mol. Pharmacol.* **48**:362–378 (1995).
13. Neve, K. A. Regulation of dopamine D_2 receptors by sodium and pH. *Mol. Pharmacol.* **39**:570–578 (1991).
14. Nunnari, J. M., M. G. Repaske, S. Brandon, E. J. Cragoe Jr., and L. E. Limbird. Regulation of porcine brain α_2-adrenergic receptors by Na^+, H^+ and inhibitors of Na^+/H^+ exchange. *J. Biol. Chem.* **262**:12387–12392 (1987).
15. Kleyman, T. R., and E. J. Cragoe, Jr. Cation transport probes: the amiloride series. *Methods Enzymol.* **191**:739–755 (1990).
16. Horstman, D. A., S. B. Brandon, A. L. Wilson, C. A. Guyer, E. J. Cragoe, Jr., and L. E. Limbird. An aspartate conserved among G-protein-coupled receptors confers allosteric regulation of α_2-adrenergic receptors by sodium. *J. Biol. Chem.* **265**:21590–21595 (1990).
17. Neve, K. A., B. A. Cox, R. A. Henningsen, A. Spanoyannis, and R. L. Neve. Pivotal role for aspartate-80 in the regulation of dopamine D_2 receptor affinity for drugs and inhibition of adenylyl cyclase. *Mol. Pharmacol.* **39**:733–739 (1991).
18. Howard, M. J., R. J. Hughes, H. J. Motulsky, M. D. Mullen, and P. A. Insel. Interactions of amiloride with α- and β- adrenergic receptors: amiloride reveals an allosteric site on α_2-adrenergic receptors. *Mol. Pharmacol.* **32**:53–58 (1987).
19. Castro, S. W., and P. G. Strange. Differences in the ligand-binding properties of the short and long versions of the D_2 dopamine receptor. *J. Neurochem.* **60**:372–375 (1993).
20. Seeman, P., C. Ulpian, K. A. Wreggett, and J. W. Wells. Dopamine receptor parameters detected by [^{3}H]spiperone depend on tissue concentration: analysis and examples. *J. Neurochem.* **43**:221–235 (1984).
21. Arunlakshana, O., and H. O. Schild. Some quantitative uses of drug antagonists. *Br. J. Pharmacol. Chemother.* **14**:48–58 (1959).
22. Vigne, P., C. Frelin, E. J. Cragoe, Jr., and M. Lazdunski. Structure-activity relationships of amiloride and certain of its analogues in relation to the blockade of the Na^+/H^+ exchange system. *Mol. Pharmacol.* **25**:131–136 (1984).
23. Garcia, M. L., F. V. King, J. L. Shevell, R. S. Slaughter, G. Suarez-Kurtz, R. J. Winquist, and G. J. Kaczorowski. Amiloride analogues inhibit L-type calcium channels and display calcium entry blocker activity. *J. Biol. Chem.* **265**:3763–3771 (1990).
24. Wilson, A. L., S. W. Womble, C. Prakash, E. J. Cragoe, Jr., I. A. Blair, and L. E. Limbird. Novel amiloride analogue allosterically modulates the α_2-adrenergic receptor but does not inhibit Na^+/H^+ exchange. *Mol. Pharmacol.* **42**:175–179 (1992).
25. Neve, K. A., M. R. Kozlowski, and M. P. Rosser. Dopamine D2 receptor stimulation of Na^+/H^+ exchange assessed by quantification of extracellular acidification. *J. Biol. Chem.* **267**:25748–25753 (1992).
26. Chio, C. L., M. E. Lajiness, and R. M. Huff. Activation of heterologously expressed D_3 dopamine receptors: comparison with D_2 dopamine receptors. *Mol. Pharmacol.* **45**:51–60 (1994).
27. Chio, C. L., R. F. Drong, D. T. Riley, G. S. Gill, J. L. Slightom, and R. M. Huff. D4 dopamine receptor-mediated signalling events determined in transfected Chinese hamster ovary cells. *J. Biol. Chem.* **269**:11813–11819 (1994).
28. Hoare, S. R. J., M. C. Coldwell, and P. G. Strange. Allosteric regulation of rat and human dopamine receptor subtypes: evidence for two binding states for [^{3}H]spiperone. *Biochem. Soc. Trans.* **24**:53S (1996).
29. Perez-Reyes, E., H. S. Kim, A. E. Lacerda, W. Horne, X. Wei, D. Rampe, K. P. Campbell, A. M. Brown, and L. Birnbaumer. Induction of calcium currents by the expression of the α_1-subunit of the dihydropyridine receptor from skeletal muscle. *Nature (Lond.)* **340**:233–236 (1989).
30. Henis, Y. I., Y. Kloog, and M. Sokolovsky. Allosteric interactions of muscarinic receptors and their regulation by other membrane proteins, in *The Muscarinic Receptors* (J. H. Brown, ed.). Humana Press, Totowa, NJ (1989).
31. Ellis, J., and M. Seidenberg. Two allosteric modulators interact at a common site on cardiac muscarinic receptors. *Mol. Pharmacol.* **42**:638–641 (1992).
32. Kenakin, T. *Pharmacologic Analysis of Drug-Receptor Interaction.* 2nd ed. Raven Press, New York, 315–318 (1993).
33. Hulme, E. C., and N. J. M. Birdsall. Strategy and tactics in receptor binding studies, in *Receptor-Ligand Interactions: A Practical Approach* (E. C. Hulme, ed.). Oxford University Press, New York (1992).
34. DeLean, A., B. F. Kilpatrick, and M. G. Caron. Dopamine receptors of the porcine anterior pituitary gland: evidence for two affinity states discriminated by both agonists and antagonists. *Mol. Pharmacol.* **22**:290–297 (1982).
35. Watanabe, M., S. R. George, and P. Seeman. Regulation of anterior pituitary D_2 dopamine receptors by magnesium and sodium ions. *J. Neurochem.* **45**:1842–1849 (1985).
36. Grigoriadis, D., and P. Seeman. Complete conversion of brain D_2 dopamine receptors from the high- to low-affinity state for dopamine agonists, using sodium ions and guanine nucleotide. *J. Neurochem.* **44**:1925–1935 (1985).
37. Wreggett, K. A., and A. DeLean. The ternary complex model: its properties and application to ligand interactions with the D_2 dopamine receptor of the anterior pituitary gland. *Mol. Pharmacol.* **26**:214–227 (1984).
38. Chatterjee, T. K., C. E. Scott, D. M. Vazquez, and R. K. Bhatnagar. Interaction of [^{3}H]spiperone with rat striatal dopamine D_2 receptors: kinetic evidence for antagonist-induced formation of ternary complex. *Mol. Pharmacol.* **33**:402–413 (1988).
39. Sato, M., R. Kataoko, J. Dingus, M. Wilcox, J. D. Hildebrandt, and S. M. Lanier. Factors determining specificity of signal transduction by G-protein-coupled receptors. *J. Biol. Chem.* **270**:15269–15276 (1995).
40. Potter, L. T., C. A. Ferrendelli, H. E. Hanchett, M. A. Hollifield, and M. V. Lorenzi. Tetrahydroaminoachridine and other allosteric antagonists of hippocampal M1 muscarinic receptors. *Mol. Pharmacol.* **35**:652–660 (1989).

Send reprint requests to: Dr. P. G. Strange, Research School of Biosciences, The University, Canterbury, CT2 7NJ, United Kingdom. E-mail: pgs@ukc.ac.uk